

# Biochemical Identification of a Linear Cholesterol-Binding Domain within Alzheimer's $\beta$ Amyloid Peptide

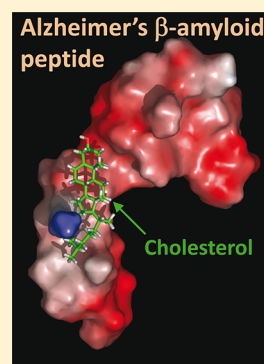
Coralie Di Scala, Nouara Yahy, Clément Lelièvre, Nicolas Garmy, Henri Chahinian, and Jacques Fantini\*

Laboratoire PPSN, EA 4674, Interactions Moléculaires et Systèmes Membranaires, Faculté des Sciences de St-Jérôme, Aix-Marseille Université, Service 331, 13331 Marseille cedex 20, France

## Supporting Information

**ABSTRACT:** Alzheimer's  $\beta$ -amyloid ( $A\beta$ ) peptides can self-organize into amyloid pores that may induce acute neurotoxic effects in brain cells. Membrane cholesterol, which regulates  $A\beta$  production and oligomerization, plays a key role in this process. Although several data suggested that cholesterol could bind to  $A\beta$  peptides, the molecular mechanisms underlying cholesterol/ $A\beta$  interactions are mostly unknown. On the basis of docking studies, we identified the linear fragment 22–35 of  $A\beta$  as a potential cholesterol-binding domain. This domain consists of an atypical concatenation of polar/apolar amino acid residues that was not previously found in cholesterol-binding motifs. Using the Langmuir film balance technique, we showed that synthetic peptides  $A\beta$ 17–40 and  $A\beta$ 22–35, but not  $A\beta$ 1–16, could efficiently penetrate into cholesterol monolayers. The interaction between  $A\beta$ 22–35 and cholesterol was fully saturable and lipid-specific. Single-point mutations of Val-24 and Lys-28 in  $A\beta$ 22–35 prevented cholesterol binding, whereas mutations at residues 29, 33, and 34 had little to no effect. These data were consistent with the *in silico* identification of Val-24 and Lys-28 as critical residues for cholesterol binding. We conclude that the linear fragment 22–35 of  $A\beta$  is a functional cholesterol-binding domain that could promote the insertion of  $\beta$ -amyloid peptides or amyloid pore formation in cholesterol-rich membrane domains.

**KEYWORDS:** Amyloid pore, cholesterol, cholesterol-binding domain, Alzheimer, lipid monolayer



According to the amyloid hypothesis,  $\beta$ -amyloid ( $A\beta$ ) peptides released upon proteolytic cleavage of the amyloid  $\beta$  A4 protein (also referred to as the amyloid precursor protein, APP) are the toxic elements causing Alzheimer's disease.<sup>1</sup> Yet the molecular and cellular mechanisms associated with the neuronal toxicity of  $A\beta$  remain elusive.<sup>2</sup> Several distinct  $A\beta$  peptides with various lengths have been shown to accumulate in the brain of Alzheimer's disease patients, forming amyloid fibrils and deposits.<sup>3,4</sup> These amyloid fibrils have long been considered as the major cause of toxicity, but smaller species such as ion channel-forming oligomers might also be harmful for neurons.<sup>5</sup>

Membrane lipids, especially sphingolipids and cholesterol, control the proteolytic cleavage of APP, which is thought to occur in lipid rafts.<sup>6</sup> Consistently, a direct association of APP with cholesterol<sup>7</sup> and gangliosides<sup>8</sup> has been demonstrated. Interestingly, recent insightful studies have shown that APP has a flexible transmembrane domain that can interact with cholesterol.<sup>9</sup> In particular, it has been suggested that membrane-buried motifs enriched in glycine residues play a critical role in the interaction of APP with cholesterol. Despite this significant breakthrough, little is known about the molecular mechanisms underlying the interaction of cholesterol with  $A\beta$  peptides. This is an important gap since (i)  $A\beta$  peptides are considered as major neurotoxic molecular species of Alzheimer's disease, (ii) high cholesterol is one of the most important risk factors for Alzheimer's disease, and (iii)  $A\beta$  peptides can interact with cholesterol.<sup>10</sup> In the present study,

we have first used a docking approach<sup>11</sup> that has led us to identify the linear fragment 22–35 of  $A\beta$ 1–40 as a potential binding site for cholesterol. Then, we have validated these *in silico* data by studying the interaction of a collection of wild-type fragments and mutant  $A\beta$  peptides with cholesterol monolayers. Although the cholesterol-binding domain of  $A\beta$  contains some of the amino acid residues previously shown to play a role in APP–cholesterol interactions,<sup>12</sup> our data showed that distinct molecular mechanisms control the binding of cholesterol to APP and to  $A\beta$  peptides. This point is carefully discussed, as well as the potential impact of cholesterol on the insertion and oligomerization process of  $A\beta$  that lead to the formation of neurotoxic amyloid pores in the plasma membrane of brain cells.

## RESULTS

**Membrane Topology of APP and  $A\beta$  Release.** The amyloid  $\beta$  A4 protein (referred to as amyloid precursor protein, APP) is a membrane protein synthesized as a single chain containing 770 amino acid residues. The first 17 residues correspond to the signal sequence. The protein encompasses a single transmembrane (TM) domain (fragment 700–723), one large extracellular domain (fragment 18–699), and a shorter cytoplasmic domain (fragment 724–770) (Figure 1). APP can

Received: November 10, 2012

Accepted: December 13, 2012

Published: December 27, 2012

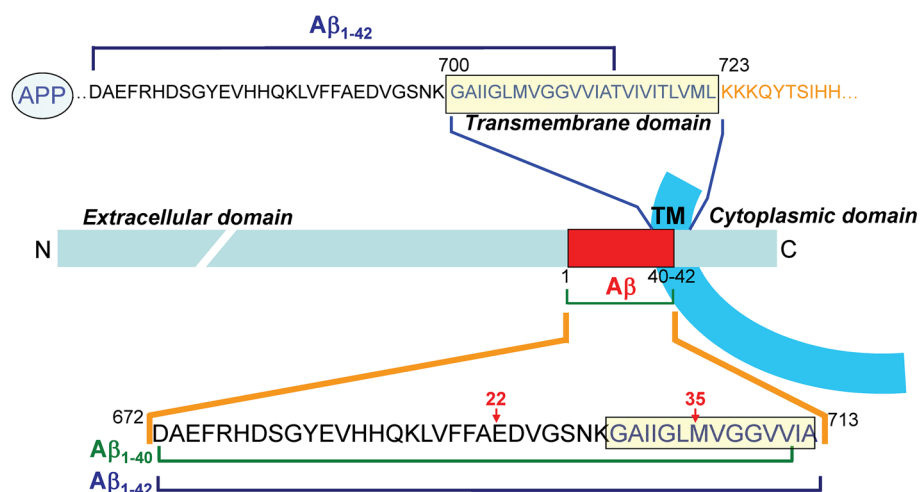


**Figure 1.** Membrane topology of APP and location of  $A\beta$  peptides. The amyloid  $\beta$  A4 protein (APP) is a transmembrane protein containing only one membrane spanning domain (transmembrane domain, TM). The N-terminal domain is extracellular, and the C-terminal domain is cytoplasmic (segment 1–17 corresponds to the signal peptide). The TM domain (700–723) is enriched in glycine, isoleucine, and valine residues. The segment of APP corresponding to the amyloid  $\beta$  peptides ( $A\beta_{1-40}$  and  $A\beta_{1-42}$ ) is indicated by a red frame in the APP chain. These peptides are generated from the proteolytic cleavage of APP by  $\beta$ -secretase (site 671–672) and  $\gamma$ -secretase (sites 711–712 and 713–714, respectively, for  $A\beta_{1-40}$  and  $A\beta_{1-42}$ ). An important feature of  $A\beta$  peptides is that they contain the N-terminal part of the initial TM domain of APP (12 or 14 amino acid residues) linked to a 28 amino acid segment belonging to the extracellular domain of APP (fragment 671–699).

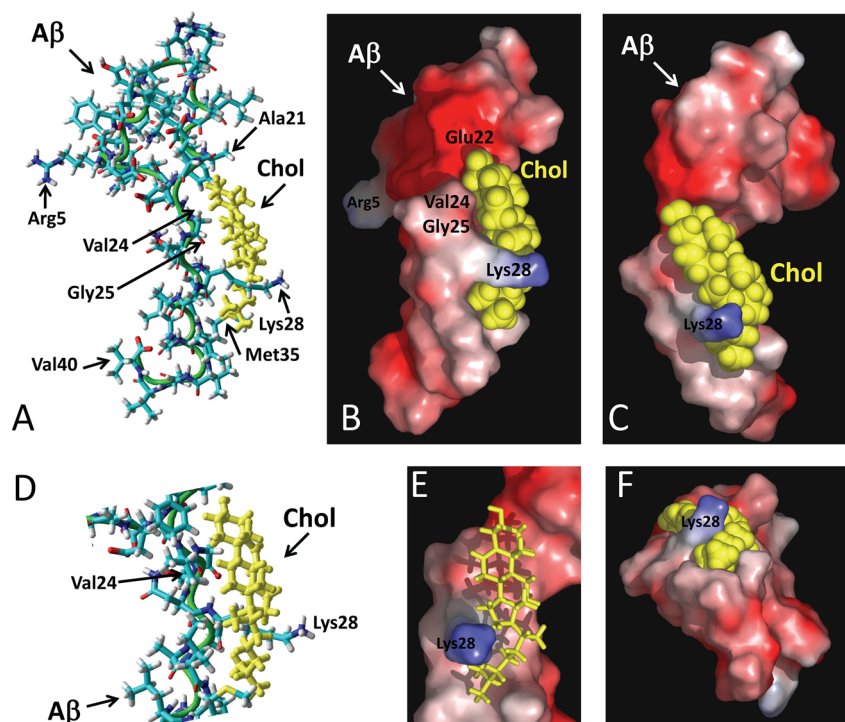


**Figure 2.** Molecular modeling simulations of cholesterol- $A\beta$  interactions. A high energy complex between  $A\beta_{1-40}$  and cholesterol was obtained by molecular dynamics simulations as explained in the Methods section. The micellar structure of  $A\beta_{1-40}$  was derived from the 1BA4 PDB entry.<sup>13</sup> After geometry optimization with the Polak–Ribiere algorithm,  $A\beta_{1-40}$  was manually merged with cholesterol in various initial orientations. Molecular dynamics simulations were then performed for 10 ps. This allowed us to obtain a complex displaying an excellent geometric complementarity between  $A\beta$  and cholesterol. This complex is shown in a tube representation, with cholesterol in yellow (A, D), and in molecular surface models (B, C, E, F). A remarkable feature of the model is the position of the side chain of Lys-28, which surrounds cholesterol in an arm-like configuration. This is particularly visible in panels B and C. The methylene groups of the lysine side chain interacts with the isoocetyl chain of cholesterol through van der Waals interactions, leaving the  $\epsilon$ - $\text{NH}_3^+$  group available for interacting with a polar environment (which could be either water molecules or negatively charged membrane lipids, for example, gangliosides). Several other van der Waals interactions involve amino acid residues in the 20–35 region of  $A\beta$  (see Table 1 for a quantitative energetic analysis of this complex).

be cleaved into as many as 14 distinct chains, of which two correspond to the  $\beta$ -amyloid proteins  $A\beta_{1-40}$  and  $A\beta_{1-42}$ . These amyloid peptides ( $A\beta$ ) are generated from proteolytic

cleavage of APP by the  $\beta$ - and  $\gamma$ -secretase at specific sites: after Met-672 for  $\beta$ -secretase and after Val-711 ( $A\beta_{1-40}$ ) or Ala-713 ( $A\beta_{1-42}$ ) for  $\gamma$ -secretase. It is important to note that Met-

672 is located in the extracellular domain of APP, whereas Val-711 and Ala-713 belong to the TM domain (Figure 1). This means that A $\beta$ 1–40 and A $\beta$ 1–42 share the same N-terminal domain and that this domain originally belonged to the extracellular part of APP. Moreover, the C-terminal domains of A $\beta$ 1–40 and A $\beta$ 1–42 contain a series of apolar amino acid residues that come from the TM domain of APP. Recent NMR data have shown that in a membrane-like micellar environment, the TM domain of APP adopts a flexible  $\alpha$ -helix structure.<sup>9</sup> However, secondary structure predictions suggest that neither the membrane-bound domain of APP nor the A $\beta$  peptides are intrinsically predetermined to form an  $\alpha$ -helix (see Supporting Information for a detailed analysis of the secondary structure of APP and A $\beta$ ). Thus, other factors such as the polarity of the environment or the presence of membrane lipids could control the balance between unfolded,  $\alpha$ , and  $\beta$  structures. Indeed, the structure of A $\beta$ 1–40 has been determined by NMR analysis of the peptide mixed with detergent micelles.<sup>13</sup> This structure contains an extended hydrophobic  $\alpha$ -helical motif formed by residues 15–36 with a hinge at residues 25–27. In this case, the membrane helps the peptide to adopt a three-dimensional structure differing from the totally disordered conformations characteristic of the peptide in water solution.<sup>13,14</sup> We used this “membrane-constrained” structure of A $\beta$  as a starting point for our docking studies.

**Molecular Dynamics Simulations of Cholesterol–A $\beta$  Interactions.** Cholesterol was merged with the micellar form of A $\beta$ 1–40 in various locations and orientations. The geometry optimization algorithm was applied for each starting condition, after which molecular dynamics simulations were conducted for iterative periods of 10 ps until a stable complex was obtained. The best fit obtained with this method is shown in Figure 2. The cholesterol-binding site of A $\beta$  was identified as a linear domain encompassing amino acids 20–35 of A $\beta$ 1–40 (i.e., APP693–706): <sup>20</sup>FAEDVGSNKGAIIGLM<sup>35</sup>. This domain of A $\beta$  forms a relatively planar surface (Figure 2D), which allows an interaction with the smooth face of cholesterol, that is, the  $\alpha$  face.<sup>2,11</sup> In this complex, the OH group of cholesterol is at a distance of 3.64 Å of the peptidic NH group of Glu-22. The complex is stabilized by numerous van der Waals interactions involving Ala-21, Val-24, Gly-25, Ile-31, Ile-32, and Met-35 (Table 1, Figure 2A,D). Moreover, the methylene groups of Lys-28 are very close to the isoctyl chain of cholesterol, allowing the establishment of several van der Waals contacts. The specific interaction between cholesterol and Lys-28 is illustrated with the surface models shown in Figure 2B,C,E,F). It is clearly visible that the side chain of Lys-28 wraps around the isoctyl tail of cholesterol in a protective fashion, leaving its charged  $\epsilon$ -NH<sub>3</sub><sup>+</sup> group available for potential interactions with polar groups (either water molecules outside the membrane or other A $\beta$  peptides inside). Overall, the apolar part of cholesterol occupies an apolar surface delineated by residues 20–35 in the structure of A $\beta$ . Interestingly, this linear domain of A $\beta$  contains several amino acid residues that have been involved in cholesterol binding to the transmembrane domain of APP, on the basis of nuclear magnetic resonance studies.<sup>7,9,12</sup> The contribution of these amino acid residues to APP–cholesterol interactions is summarized in Table 1. In our docking study, the total energy of interaction between cholesterol and A $\beta$ 1–40 could be estimated to  $-76.9$  kJ·mol<sup>-1</sup>.

**Physicochemical Studies of A $\beta$ –Cholesterol Interactions.** In order to evaluate the reliability of our docking study, we analyzed the interaction of a collection of synthetic A $\beta$

**Table 1. Energetics of Interaction of Cholesterol with A $\beta$  and APP**

amino acid residue in APP and in A $\beta$ <sup>a</sup>	A $\beta$ –cholesterol $\Delta G^b$ (kJ·mol <sup>-1</sup> )	C99 in LMPG/cholesterol analogue micelles <sup>c</sup> (%)	C99 in DMPC/cholesterol micelles <sup>d</sup> (%)
Val-689 (A $\beta$ -18)		10	
Phe-690 (A $\beta$ -19)		20	12
Phe-691 (A $\beta$ -20)	-0.525	6	30
Ala-692 (A $\beta$ -21)	-7.620	25	
Glu-693 (A $\beta$ -22)	-5.754		50
Asp-694 (A $\beta$ -23)	-2.034		
Val-695 (A $\beta$ -24)	-16.097	12	
Gly-696 (A $\beta$ -25)	-7.387	100	25
Ser-697 (A $\beta$ -26)		65	25
Asn-698 (A $\beta$ -27)			40
Lys-699 (A $\beta$ -28)	-18.894	50	2
Gly-700 (A $\beta$ -29)		25	90
Ala-701 (A $\beta$ -30)		12	20
Ile-702 (A $\beta$ -31)	-9.663		20
Ile-703 (A $\beta$ -32)	-3.649		4
Gly-704 (A $\beta$ -33)			100
Leu-705 (A $\beta$ -34)			
Met-706 (A $\beta$ -35)	-5.302	16	18
Val-707 (A $\beta$ -36)			
Gly-708 (A $\beta$ -37)			25
Gly-709 (A $\beta$ -38)			18
Val-710 (A $\beta$ -39)			50
Val-711 (A $\beta$ -40)		9	

<sup>a</sup>APP is numbered from 1 to 770 and A $\beta$  from 1 to 40. To facilitate the conversion between both numbering systems, the correspondence of each APP amino acid residue in A $\beta$  is indicated in parentheses. <sup>b</sup>Energy of interaction as determined by molecular docking in the present study. <sup>c</sup>Calculated from the data of Beel et al.,<sup>12</sup> the numbers indicate the percentage of chemical shift relative to the maximal chemical shift value taken as 100% (Gly-625 in this case). <sup>d</sup>Calculated from the data of Barrett et al.,<sup>9</sup> with the 100% corresponding to the chemical shift of Gly-704. C99 is the 99-residue transmembrane C-terminal domain of APP liberated by  $\beta$ -secretase cleavage. LMPG, lyso-myristoylphosphatidylglycerol; DMPC, dimyristoyl-phosphatidylcholine.

peptides with cholesterol using the Langmuir film balance technique.<sup>15</sup> The peptides used were A $\beta$ 1–11, A $\beta$ 1–16, A $\beta$ 5–16, A $\beta$ 17–40, A $\beta$ 20–35, and A $\beta$ 22–35. As shown in Figure 3A, the interaction was very efficient with the peptides containing the predicted cholesterol-binding domain (i.e., A $\beta$ 17–40, A $\beta$ 20–35, and A $\beta$ 22–35) and weak with peptide fragments outside this domain (i.e., A $\beta$ 1–11, A $\beta$ 1–16, A $\beta$ 5–16). In these experiments, cholesterol was spread on the surface of a water meniscus, and after equilibration of the monolayer, the synthetic peptide was injected in the subphase at a final concentration of 10  $\mu$ M. The interaction of each A $\beta$  peptide with cholesterol was quantified by measuring in real-time the changes of the surface pressure of the monolayer. This is illustrated in the kinetic experiment of Figure 3B, where A $\beta$ 22–35 induced a rapid surface pressure increase of the cholesterol monolayer, indicating an efficient insertion of the peptide between cholesterol molecules. Interestingly, A $\beta$ 22–35 ap-

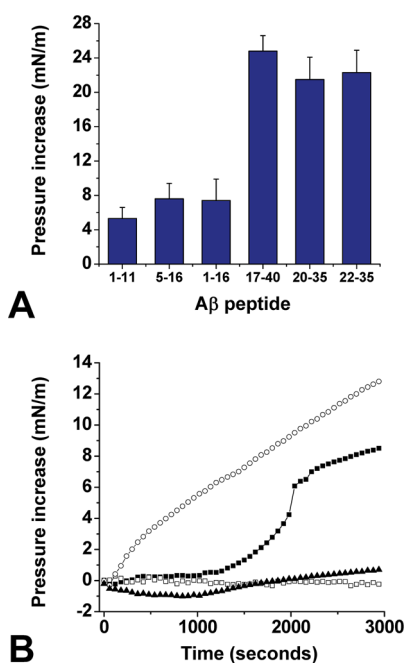


**Figure 3.** Identification of  $A\beta_{22-35}$  as a lipid-specific cholesterol-binding motif. (A) Structure–activity study of  $A\beta$ –cholesterol interactions. The indicated synthetic  $A\beta$  fragment was injected underneath a monolayer of cholesterol prepared at an initial surface pressure  $\pi_i$  of  $15 \text{ mN}\cdot\text{m}^{-1}$ . After reaching equilibrium, the maximal surface pressure increase was recorded. The data are expressed as the mean  $\pm$  SD ( $n = 3$ ). (B) Kinetics studies of  $A\beta_{22-35}$  interaction with monolayers of cholesterol (O), POPC (■), sphingomyelin (□), or GM1 (▲). The data show the real-time changes of surface pressure following injection of  $10 \mu\text{M}$   $A\beta_{22-35}$  beneath each lipid monolayer prepared at an initial surface pressure of  $20 \text{ mN}\cdot\text{m}^{-1}$ . Each curve is representative of three separate experiments (SD < 10%).

peared to be as efficient as the larger peptides  $A\beta_{17-40}$  and  $A\beta_{20-35}$  for cholesterol binding. Thus, this minimal cholesterol-binding peptide was used for further physicochemical characterization of  $A\beta$ –cholesterol interactions.

One important issue was to assess the biochemical specificity of  $A\beta_{22-35}$  for cholesterol. Therefore, we studied the interaction of  $A\beta_{22-35}$  with various lipid monolayers. We observed that in marked contrast with cholesterol, the peptide did not significantly interact with monolayers of sphingomyelin (SM) or ganglioside GM1. However,  $A\beta_{22-35}$  could interact with a monolayer of palmitoyl-oleoyl-phosphatidylcholine (POPC), although after a significant lag phase (Figure 3B). Moreover, the maximal surface pressure increase ( $\Delta\pi_{\text{max}}$ ) was reached after 1 h of incubation with POPC monolayer, whereas at this time it still increased for cholesterol. Overall these data indicated that  $A\beta_{22-35}$  has a high affinity for cholesterol, a moderate affinity for POPC, and no affinity at all for SM and GM1. Moreover, when various concentrations of  $A\beta_{22-35}$  were added underneath the cholesterol monolayer, a dose-dependent response was recorded, which further demonstrated the specificity of the peptide for cholesterol (Figure 4A). The half-saturation was obtained for  $1 \mu\text{M}$  of  $A\beta_{22-35}$ . Finally, in order to measure the avidity of  $A\beta_{22-35}$  for cholesterol, experiments were performed with cholesterol monolayers prepared at various values of the surface pressure (initial surface pressure,  $\pi_i$ ). The data are expressed as  $\Delta\pi_{\text{max}} = f(\pi_i)$  curves. As shown in Figure 4B, the values of  $\Delta\pi_{\text{max}}$  gradually decreased as  $\pi_i$  increased, which demonstrates the specificity of

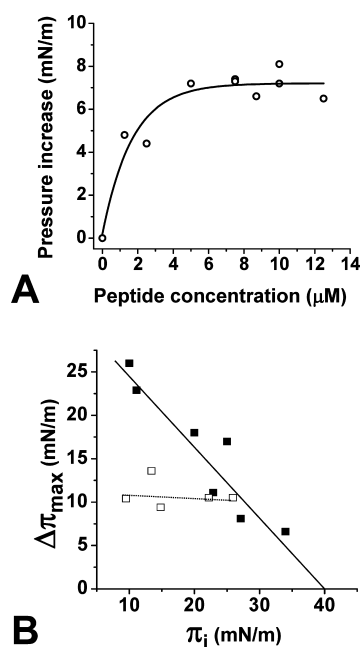


**Figure 4.** Physicochemical parameters of  $A\beta_{22-35}$  interaction with cholesterol monolayers. (A) Interaction of  $A\beta_{22-35}$  added at different concentrations underneath a cholesterol monolayer. In each case, the surface pressure increase was determined after 30 min of interaction. (B) Specificity of cholesterol– $A\beta_{22-35}$  interaction. Cholesterol monolayers were prepared at various values (initial surface pressure range  $10\text{--}34 \text{ mN}\cdot\text{m}^{-1}$ ). After equilibration of the monolayer,  $A\beta_{1-16}$  (□) or  $A\beta_{22-35}$  (■) were added in the subphase at a final concentration of  $10 \mu\text{M}$ . The maximal surface pressure increase ( $\Delta\pi_{\text{max}}$ ) was measured after reaching equilibrium. The critical pressure of insertion was extrapolated as the value of the initial surface pressure at  $\Delta\pi_{\text{max}} = 0$ .

the interaction. These experiments also allowed us to determine the critical pressure of insertion ( $\pi_c$ ) of the protein for the monolayer as the extrapolated value of  $\pi_i$  at  $\Delta\pi_{\text{max}} = 0$ . It represents the surface pressure of the monolayer above which no further interaction occurs, because the lipids are too densely packed. The value of  $\pi_c$  was estimated at  $41 \text{ mN}\cdot\text{m}^{-1}$ , which is above the threshold value of  $30 \text{ mN}\cdot\text{m}^{-1}$  measured in vivo for a real plasma membrane.<sup>16</sup> For the sake of comparison, we analyzed under similar conditions the interaction of  $A\beta_{1-16}$  with cholesterol, a peptide previously shown to bind to selected glycosphingolipids.<sup>17</sup> In this case,  $\Delta\pi_{\text{max}}$  remained constant whatever the value of  $\pi_i$  was (Figure 4B). This behavior indicates that  $A\beta_{1-16}$  can loosely bind to the surface of the cholesterol monolayer, without inserting between cholesterol molecules. Overall these data indicated that  $A\beta_{22-35}$  is able to efficiently penetrate a cholesterol monolayer. Thus, this short linear fragment of  $A\beta$  can be considered as a functional cholesterol-binding domain.

**Mutations in  $A\beta_{22-35}$  Affect Cholesterol Recognition.** According to our docking studies, two amino acid residues appeared to have a critical role in the interaction of  $A\beta_{22-35}$  with cholesterol: Val-24 and Lys-28, which contribute, respectively, 23.4% and 27.5% of the total energy of interaction ( $-68.8 \text{ kJ}\cdot\text{mol}^{-1}$  for  $A\beta_{22-35}$ ). Thus, we evaluated the impact of single-point substitutions at these key positions. When the synthetic mutant peptides  $A\beta_{22-35}/\text{Val24Gly}$ ,  $A\beta_{22-35}/\text{Lys28Gly}$ , or  $A\beta_{22-35}/\text{Lys28Arg}$  were injected underneath cholesterol monolayers ( $\pi_i$  of  $20 \text{ mN}\cdot\text{m}^{-1}$ ),



only minor increases of the surface pressure were recorded compared with the wild-type A $\beta$ 22–35 peptide (Figure 5A).

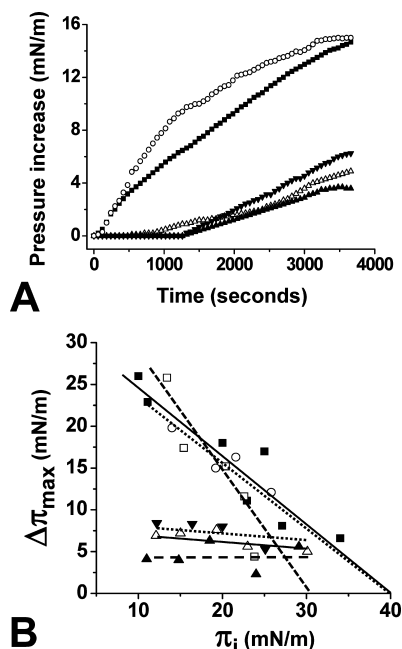


**Figure 5.** Effect of single-point and double mutations on the insertion of A $\beta$ 22–35 within cholesterol monolayers. (A) Cholesterol monolayers ( $\pi_i = 20 \text{ mN}\cdot\text{m}^{-1}$ ) were incubated with wild-type (■), Val24Gly (▲), Lys28Gly (△), Lys28Arg (▼), or Gly29Ala (○) A $\beta$ 22–35 peptides ( $10 \mu\text{M}$ ), and the surface pressure increases were recorded as a function of time. Each curve is representative of three separate experiments (SD < 10%). (B) Cholesterol monolayers were prepared at various  $\pi_i$  values (initial surface pressure range 10–34  $\text{mN}\cdot\text{m}^{-1}$ ). After equilibration of the monolayer, wild-type (■), Val24Gly (▲), Lys28Gly (△), Lys28Arg (▼), Gly29Ala (○), or Gly33Ala/Leu34Ala (□) A $\beta$ 22–35 peptides were added in the subphase at a final concentration of  $10 \mu\text{M}$ . The maximal surface pressure increase ( $\Delta\pi_{\max}$ ) was measured after reaching equilibrium.

Similar experiments were then performed with cholesterol monolayers prepared at various values of  $\pi_i$ , and  $\Delta\pi_{\max}$  was determined in each case (Figure 5B). The data showed that all these mutations strongly decreased the interaction of A $\beta$ 22–35 with cholesterol. Indeed, the mutant peptides were no longer able to penetrate within the cholesterol monolayer and remained loosely attached on the surface of the membrane, so that the value of  $\Delta\pi_{\max}$  was very low at all  $\pi_i$  tested, compared with the values obtained with wild-type A $\beta$ 22–35. Overall, these data indicated that cholesterol recognition by A $\beta$ 22–35 is highly dependent on the amino acid sequence of the motif and confirmed the prominent role of Val-24 and Lys-28 in cholesterol binding. As expected, mutations at other positions had little or no effect on cholesterol recognition. The A $\beta$ 22–35/Gly29Ala peptide behaved almost as the wild-type peptide, with kinetics of insertion within the cholesterol monolayer (Figure 5A) and critical pressure of insertion (Figure 5B) similar to those of the wild-type A $\beta$ 22–35 peptide. Finally, a double mutant A $\beta$ 22–35/Gly33Ala/Leu34Ala was also tested. The insertion of this double mutant in cholesterol monolayers regularly decreased as a function of  $\pi_i$ , indicating a specific interaction with cholesterol. The critical pressure of insertion of this mutant peptide was estimated to  $32 \text{ mN}\cdot\text{m}^{-1}$ , which has to be compared with  $41 \text{ mN}\cdot\text{m}^{-1}$  for the wild-type

A $\beta$ 22–35 peptide (Figure 5B). Thus, although the double mutation induced some decrease in binding affinity, it did not abolish the cholesterol-binding properties of the peptide. Taken together, these data indicated that Val-24 and Lys-28 of A $\beta$ 22–35 are critically involved in cholesterol binding, whereas residues Gly-29, Gly-33, and Leu-34 have little to no effect on the interaction.

## DISCUSSION

Although high cholesterol has been clearly identified as a major risk factor for Alzheimer's disease, little is known about the molecular mechanisms underlying the cholesterol–Alzheimer's disease connection. Several lines of evidence suggest that cholesterol directly interacts with both APP and A $\beta$  peptides: (i) the presence of APP in cholesterol-dependent microdomains,<sup>18</sup> (ii) the preferential binding of A $\beta$  peptides to glycosphingolipids (such as ganglioside GM1), which are known to be associated with cholesterol in neuronal plasma membranes,<sup>19,20</sup> (iii) the binding of cholesterol to A $\beta$  fibrils,<sup>21</sup> and (iv) the demonstration of a physical interaction between cholesterol and APP in a micellar environment.<sup>9</sup>

In this study, we used a combination of *in silico*, biochemical, and physicochemical approaches that allowed us to identify a minimal cholesterol-binding domain in Alzheimer's A $\beta$  peptides. This domain consists of a linear segment of 14 amino acid residues located in the C-terminal region of A $\beta$ 1–40, that is, A $\beta$ 22–35: EDVGSNKGAIIGLM. Of these 14 residues, 8 are directly involved in van der Waals contacts with cholesterol, thereby generating a high energy of interaction ( $-68.8 \text{ kJ}\cdot\text{mol}^{-1}$ ). Interestingly, this cholesterol-binding motif does not contain the typical biochemical features of the previously characterized linear cholesterol-binding domain including the CRAC<sup>22</sup> and CARC<sup>23</sup> consensus sequences. In particular, it is devoid of the aromatic residues that classically stack onto the sterane rings of cholesterol.<sup>24</sup> Moreover, it is not based on the classical amphipathic structure with a large apolar domain interacting with the apolar part of cholesterol and a smaller polar head that accommodates its polar OH group.<sup>23</sup> Instead, the cholesterol-binding domain of A $\beta$  consists in a regular succession of polar and apolar segments (polar<sup>22</sup> Glu-Asp<sup>23</sup>, apolar<sup>24</sup> Val-Gly<sup>25</sup>, polar<sup>26</sup> Ser-Asn-Lys<sup>28</sup>, apolar<sup>29</sup> Gly-Ala-Ile-Ile-Gly-Leu-Met<sup>35</sup>). Thus, it is an atypical and newly described cholesterol-binding domain, which displays some of the structural features of an amphipathic helix.

The cholesterol-binding properties of this new domain have been carefully assessed with the Langmuir film balance technique. This technique, which requires very low concentrations of protein (nanomolar to micromolar range), has successfully been used to determine the physicochemical parameters underlying the interaction of amyloidogenic proteins with various membrane lipids including POPC, cholesterol, and sphingolipids.<sup>11,15,17,19,25</sup> In the present study, we showed that synthetic A $\beta$  peptides containing the minimal 22–35 core motif could specifically interact with a monolayer of cholesterol. The interaction of A $\beta$ 22–35 with cholesterol was dose-dependent, saturable, and lipid-specific. In contrast, synthetic A $\beta$  derived from the N-terminal domain (A $\beta$ 1–11, A $\beta$ 1–16, A $\beta$ 5–16) did not significantly penetrate into cholesterol monolayers. A $\beta$ 22–35 exhibited a critical pressure of insertion of  $41 \text{ mN}\cdot\text{m}^{-1}$  for cholesterol monolayers (Figure 4). Interestingly, this value is close to the one obtained with a synthetic peptide derived from the cholesterol-binding domain of the Parkinson's disease associated  $\alpha$ -synuclein, that

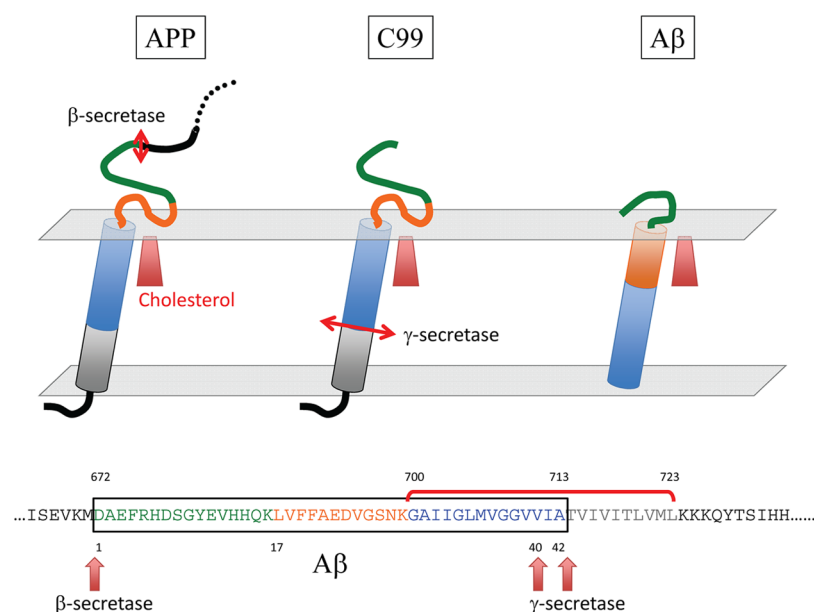


**Figure 6.** Membrane topology of APP and A $\beta$ 1–40 bound to cholesterol.

is,  $37.5 \text{ mN}\cdot\text{m}^{-1}$ .<sup>11</sup> Such high values of the critical pressure of insertion indicate that these peptides can penetrate into densely packed lipid domains,<sup>26</sup> a process that in this peculiar case requires the destabilization of cholesterol–cholesterol contacts in the membrane and their subsequent replacement by peptide–cholesterol interactions.<sup>11</sup>

It should be noted that the cholesterol-binding domain of A $\beta$  identified in the present study contains the fragment 25–35 (GSNKGAIIGLM), which is highly lipophilic and has been shown to insert into the apolar core of the membrane<sup>27</sup> through a mechanism particularly sensitive to membrane cholesterol levels.<sup>28</sup> That cholesterol could physically interact with a motif containing such a lipophilic segment is not totally unexpected. Moreover, even if the same lysine residue (Lys-699/Lys-28) can be involved in both cholesterol–APP<sup>7,12</sup> and cholesterol–A $\beta$  complexes (this study), this basic residue plays distinct roles in the interaction. For APP, it interacts with the OH group of cholesterol,<sup>7</sup> whereas in the case of A $\beta$  its methylene groups wrap around the apolar part of the cholesterol molecule for which it provides a protective apolar nest (Figure 2). This is reminiscent to the “snorkeling” effect of lysine residues in the polar–apolar interface of the plasma membrane.<sup>29</sup> The specificity of A $\beta$ 22–35 binding to cholesterol was assessed with several mutant peptides. Indeed, single-point mutations of Lys-28 (Lys28Gly and Lys28Arg) abolished the interaction of A $\beta$ 22–35 with cholesterol (Figure 5). Similarly, the intimate van der Waals contact between cholesterol and Val-24 appeared to be critical for cholesterol recognition, since the mutant A $\beta$ 22–35/Val24Gly peptide no longer interacted with cholesterol. In contrast, the other mutant peptides tested (A $\beta$ 22–35/Gly29Ala and the double mutant A $\beta$ 22–35/Gly33Ala/Leu34Ala) could still interact with cholesterol. Therefore, these physicochemical studies with mutant peptides fully confirmed the critical role of Val-24 and Lys-28 in the molecular interaction between cholesterol and A $\beta$ 22–35.

During the last years, others have attempted to define the cholesterol-binding motif on the A $\beta$  peptide. On one hand, Zhou and Xu<sup>30</sup> have performed a series of molecular dynamics simulations of the A $\beta$ 42 peptide in presence of free cholesterol. These authors focused their study on the stacking interaction

between the aromatic side chain of Phe-19 and the flat surface of cholesterol. They showed that cholesterol could attract A $\beta$  peptides on the surface of mixed sphingomyelin/cholesterol micelles and induce  $\beta$ -sheet formation and fibrillogenesis. Interestingly, this effect was no longer observed when Phe-19 was substituted with serine, suggesting that the aromatic side chain of Phe-19 is critical for cholesterol binding. Although our study did not identify Phe-19 as part of the membrane cholesterol-binding domain of A $\beta$ , we do not exclude that this aromatic residue could play a role in the association between A $\beta$  peptides and the extracellular surface of cholesterol-enriched plasma membrane domains. The frequent presence of aromatic residues in juxtamembrane cholesterol-binding sites<sup>23</sup> and the key role of the hydrophobic sequence A $\beta$ 17–21 in A $\beta$  aggregation<sup>31</sup> are in line with this hypothesis. On the other hand, the group of C. Sanders has recently published two seminal NMR studies of APP–cholesterol interactions.<sup>9,12</sup> These authors have successfully incorporated C99, the 99-residue transmembrane C-terminal domain of APP generated by  $\beta$ -secretase cleavage, in mixed micelles containing either a cholesterol analogue and lyso-myristoylphosphatidylglycerol (LMPG)<sup>12</sup> or cholesterol and dimyristoyl-phosphatidylcholine (DMPC).<sup>9</sup> Chemical shift changes between cholesterol-free and cholesterol-containing micelles allowed these authors to identify the amino acid residues involved in cholesterol binding. In both cases (LMPG and DMPC micelles), the cholesterol-binding site of APP included a part of the transmembrane domain (residues 700–711) but also interfacial residues belonging to the extracellular domain (residues 689–699). In A $\beta$ 1–40, all these amino acid residues are located in the C-terminal domain 18–40, which is in full agreement with our study of A $\beta$ –cholesterol interactions (Figure 1, Table 1, and Figure 6). Nevertheless, there are some discrepancies between the data obtained with C99 and with A $\beta$  peptides. A major outcome of the studies performed with C99 is that the transmembrane domain of APP is highly flexible and can finely modulate its 3D structure to accommodate distinct cholesterol conformers. Indeed, different data have been obtained (Table 1) according to the nature of the carrier lipid in which C99 was micellized.<sup>7,9,12</sup> For instance, Gly-696 and Lys-699 were the

most important cholesterol-binding residues of C99 in LMPG micelles.<sup>7,12</sup> However, these residues played a minor role in cholesterol binding to C-99 in DMPC micelles, whereas Gly-700 and Gly-704 were strongly involved in this case.<sup>9</sup> This versatility of cholesterol interaction is inherent to the abundance of glycine residues, which probably confer a high flexibility to the transmembrane domain of APP.<sup>9</sup> However, in the case of A $\beta$ , neither Gly-29 nor Gly-33 appeared to play a major role in cholesterol recognition, as assessed by the analysis of the cholesterol insertion capability of A $\beta$ 22–35 mutants Gly29Ala and Gly33Ala (Figure 5).

It is difficult to compare the NMR analysis<sup>9,12</sup> and our own study because we used distinct proteins at different concentrations, various membrane models, and different technological approaches. Strikingly, both studies were remarkably convergent because we located the respective cholesterol-binding domains of APP and A $\beta$  in approximately the same region, that is, APP689–711 and A $\beta$ 22–35 (Table 1). Nevertheless, the key amino acid residues controlling the binding of cholesterol were not the same in APP and A $\beta$ , indicating that each protein has its own special way to interact with cholesterol. The distinct environments to which APP and A $\beta$  are submitted could explain this molecular specificity. A $\beta$  peptides are generated from the proteolytic cleavage of APP and then released in the extracellular milieu where they can adopt a myriad of conformations. Secondary structure predictions showed that the A $\beta$ 1–40 peptide has a higher propensity to form a  $\beta$ -strand than an  $\alpha$ -helix (Supporting Information). This type of  $\alpha/\beta$  discordance has been recognized as a key feature of amyloidogenic core motifs.<sup>32</sup> When proteins containing such  $\alpha/\beta$  discordant motifs interact with membrane lipids, they are forced to adopt a helical structure.<sup>33</sup> This is the case for A $\beta$  whose  $\alpha$ -helical content increases with the percentage of cholesterol in model membranes.<sup>34</sup> As a matter of fact, the sudden insertion of extracellular A $\beta$ 1–40 within cholesterol-rich domains might involve specific amino acid residues that did not mediate the binding of APP to cholesterol. In other words, although the cholesterol-binding site of APP is also present in A $\beta$ 1–40, our study suggested that A $\beta$ 1–40 does not bind cholesterol as APP does (Figure 6). In particular, our modeling studies suggested that several amino acid residues that lie outside the membrane in APP (i.e., residues 22–28) could be part of the transmembrane domain of A $\beta$ 1–40 (residues 22–40). By exerting specific conformational effects on A $\beta$  in the exofacial leaflet of the plasma membrane, cholesterol could restrict the flexibility of the peptide and determine a topology (Figure 6) compatible with the formation of an amyloid pore through the oligomerization of several cholesterol–A $\beta$  subunits. In support of this view, recent data have shown that membrane cholesterol could both stimulate the formation and increase the activity of A $\beta$  ion channels in planar lipid membranes.<sup>35</sup>

In conclusion, we have identified and characterized the 22–35 fragment of A $\beta$  as a minimal, atypical, and functional cholesterol-binding domain. This domain could promote the insertion of A $\beta$  within cholesterol-containing membranes, as recently postulated on the basis of molecular dynamics simulation studies.<sup>36</sup> Overall, our data may provide a biochemical link between high cholesterol and Alzheimer's disease.<sup>37</sup>

## METHODS

**General.** Synthetic wild-type peptides A $\beta$ 1–11, A $\beta$ 1–16, A $\beta$ 5–16, A $\beta$ 17–40, and A $\beta$ 22–35 were purchased from rPeptide (Bogart, GA). The synthetic wild-type peptides A $\beta$ 5–16 and A $\beta$ 20–35 and the mutant peptides A $\beta$ 22–35 were obtained from Schafer-N (Copenhagen, Denmark). The purity of all peptides was >95%. Ultrapure apyrogenic water was from Biorad (Marnes La Coquette, France). All lipids were purchased from Matreya (Pleasant Gap, PA). The lipids were dissolved in hexane/chloroform/ethanol (11:5:4, vol/vol/vol) at a stock concentration of 1 mg·mL<sup>-1</sup> and stored at –20 °C under saturated nitrogen atmosphere. All experiments were carried out in a controlled atmosphere at 20 ± 1 °C.

**In Silico Studies of A $\beta$ –Cholesterol Interactions.** The amino acid sequences of human APP and A $\beta$  peptides were retrieved from the Swiss-Prot entry P05067.<sup>38</sup> The starting structure of A $\beta$ 1–40 was derived from a NMR structure of the peptide in solution in a water–micelle environment,<sup>13</sup> using the PDB entry 1BA4. To generate peptide–cholesterol complexes, one cholesterol molecule was positioned in the vicinity of the peptide (manual search for geometric fit). Several initial conditions were tested (with distinct orientations of cholesterol with respect to the peptide) to select the complex having the highest energy of interaction. Geometry optimization of each cholesterol–peptide complex was first achieved using the unconstrained optimization rendered by the Polak–Ribière conjugate gradient algorithm.<sup>11</sup> Molecular dynamics simulations were then performed for various periods of times ranging from 10 ps to 1 ns in vacuo with the Bio+ (CHARMM) force field<sup>39</sup> of the Hyperchem software suite (ChemCad, Obernay, France). The energy of interaction was determined with the Molegro Molecular Viewer.<sup>40</sup>

**Lipid Monolayer Assay.** Peptide–lipid interactions were studied with the Langmuir film balance technique.<sup>15</sup> The surface pressure,  $\pi$ , of lipid monolayers<sup>11</sup> was measured with a fully automated microtensiometer ( $\mu$ TROUGH SX, Kibron Inc. Helsinki, Finland) and calculated from the surface tension,  $\gamma$ , according to the equation [ $\pi = \gamma_0 - \gamma$ ] where  $\gamma_0$  is the observed surface tension at the air–water interface in the absence of peptide or lipid. Monomolecular films of the indicated lipid were spread on ultrapure water subphases totally devoid of any surfactant contaminant as described previously.<sup>11,19,25</sup> After spreading of the film, 5 min was allowed for solvent evaporation. The peptide was injected in the subphase (pH 7) with a 10- $\mu$ L Hamilton syringe, and pressure increases produced were continuously recorded as a function of time. The data were analyzed with the FilmWareX 3.57 program (Kibron Inc.). The accuracy of the system under our experimental conditions was  $\pm 0.25$  mN·m<sup>-1</sup> for surface pressure.

## ASSOCIATED CONTENT

### Supporting Information

Secondary structure predictions of APP and A $\beta$ . This material is available free of charge via the Internet at <http://pubs.acs.org>.

## AUTHOR INFORMATION

### Corresponding Author

\*Tel: +33 491 288 761. E-mail: [jacques.fantini@univ-amu.fr](mailto:jacques.fantini@univ-amu.fr).

### Notes

The authors declare no competing financial interest.

## ABBREVIATIONS

A $\beta$ , Alzheimer's  $\beta$ -amyloid peptide; APP, amyloid precursor protein; NMR, nuclear magnetic resonance;  $\Delta\pi_{\max}$ , maximal surface pressure increase;  $\pi_c$ , critical pressure of insertion;  $\pi_i$ , initial surface pressure

## REFERENCES

(1) Hardy, J. A., and Higgins, G. A. (1992) Alzheimer's disease: The amyloid cascade hypothesis. *Science* 256, 184–185.



- (2) Fantini, J., and Yahi, N. (2010) Molecular insights into amyloid regulation by membrane cholesterol and sphingolipids: Common mechanisms in neurodegenerative diseases. *Expert Rev. Mol. Med.* 12, No. e27.
- (3) Naslund, J., Schierhorn, A., Hellman, U., Lannfelt, L., Roses, A. D., Tjernberg, L. O., Silberring, J., Gandy, S. E., Winblad, B., Greengard, P., Norstedt, C., and Terenius, L. (1994) Relative abundance of Alzheimer A $\beta$  amyloid peptide variants in Alzheimer disease and normal aging. *Proc. Natl. Acad. Sci. U.S.A.* 91, 8378–8382.
- (4) Harigaya, Y., Saido, T. C., Eckman, C. B., Prada, C. M., Shoji, M., and Younkin, S. G. (2000) Amyloid beta protein starting pyroglutamate at position 3 is a major component of the amyloid deposits in the Alzheimer's disease brain. *Biochem. Biophys. Res. Commun.* 276, 422–427.
- (5) Butterfield, S. M., and Lashuel, H. A. (2010) Amyloidogenic protein-membrane interactions: mechanistic insight from model systems. *Angew. Chem., Int. Ed.* 49, 5628–5654.
- (6) Vetrivel, K. S., and Thinakaran, G. (2010) Membrane rafts in Alzheimer's disease beta-amyloid production. *Biochim. Biophys. Acta* 1801, 860–867.
- (7) Beel, A. J., Sakakura, M., Barrett, P. J., and Sanders, C. R. (2010) Direct binding of cholesterol to the amyloid precursor protein: An important interaction in lipid-Alzheimer's disease relationships? *Biochim. Biophys. Acta* 1801, 975–982.
- (8) Zhang, H., Ding, J., Tian, W., Wang, L., Huang, L., Ruan, Y., Lu, T., Sha, Y., and Zhang, D. (2009) Ganglioside GM1 binding the N-terminus of amyloid precursor protein. *Neurobiol. Aging* 30, 1245–1253.
- (9) Barrett, P. J., Song, Y., Van Horn, W. D., Hustedt, E. J., Schafer, J. M., Hadziselimovic, A., Beel, A. J., and Sanders, C. R. (2012) The amyloid precursor protein has a flexible transmembrane domain and binds cholesterol. *Science* 336, 1168–1171.
- (10) Valdes-Gonzalez, T., Inagawa, J., and Ido, T. (2001) Neuropeptides interact with glycolipid receptors: A surface plasmon resonance study. *Peptides* 22, 1099–1106.
- (11) Fantini, J., Carlus, D., and Yahi, N. (2011) The fusogenic tilted peptide (67–78) of  $\alpha$ -synuclein is a cholesterol binding domain. *Biochim. Biophys. Acta* 1808, 2343–2351.
- (12) Beel, A. J., Mobley, C. K., Kim, H. J., Tian, F., Hadziselimovic, A., Jap, B., Prestegard, J. H., and Sanders, C. R. (2008) Structural studies of the transmembrane C-terminal domain of the amyloid precursor protein (APP): Does APP function as a cholesterol sensor? *Biochemistry* 47, 9428–9446.
- (13) Coles, M., Bicknell, W., Watson, A. A., Fairlie, D. P., and Crai, D. J. (1998) Solution structure of amyloid  $\beta$ -peptide(1–40) in a water-micelle environment. Is the membrane-spanning domain where we think it is? *Biochemistry* 37, 11064–11077.
- (14) Shao, H., Jao, S., Ma, K., and Zagorski, M. G. (1999) Solution structures of micelle-bound amyloid beta-(1–40) and beta-(1–42) peptides of Alzheimer's disease. *J. Mol. Biol.* 285, 755–773.
- (15) Thakur, G., Mivic, M., and Leblanc, R. M. (2009) Surface chemistry of Alzheimer's disease: A Langmuir monolayer approach. *Colloids Surf., B* 74, 436–456.
- (16) Seelig, A. (1987) Local anesthetics and pressure: A comparison of dibucaine binding to lipid monolayers and bilayers. *Biochim. Biophys. Acta* 899, 196–204.
- (17) Di Pasquale, E., Fantini, J., Chahinian, H., Maresca, M., Taieb, N., and Yahi, N. (2010) Altered ion channel formation by the Parkinson's-disease-linked E46K mutant of alpha-synuclein is corrected by GM3 but not by GM1 gangliosides. *J. Mol. Biol.* 397, 202–218.
- (18) Sakurai, T., Kaneko, K., Okuno, M., Wada, K., Kashiyama, T., Shimizu, H., Akagi, T., Hashikawa, T., and Nukina, N. (2008) Membrane microdomain switching: A regulatory mechanism of amyloid precursor protein processing. *J. Cell Biol.* 183, 339–352.
- (19) Yahi, N., Aulas, A., and Fantini, J. (2010) How cholesterol constrains glycolipid conformation for optimal recognition of Alzheimer's beta amyloid peptide (A $\beta$ 1–40). *PLoS One* 5, No. e9079.
- (20) Matsuzaki, K., Kato, K., and Yanagisawa, K. (2010) Abeta polymerization through interaction with membrane gangliosides. *Biochim. Biophys. Acta* 180, 868–877.
- (21) Harris, J. R. (2008) Cholesterol binding to amyloid-beta fibrils: A TEM study. *Micron* 39, 1192–1196.
- (22) Jamin, N., Neumann, J. M., Ostuni, M. A., Vu, T. K., Yao, Z. X., Murail, S., Robert, J. C., Giatzakis, C., Papadopoulos, V., and Lacapère, J. J. (2005) Characterization of the cholesterol recognition amino acid consensus sequence of the peripheral-type benzodiazepine receptor. *Mol. Endocrinol.* 19, 588–594.
- (23) Baier, C. J., Fantini, J., and Barrantes, F. J. (2011) Disclosure of cholesterol recognition motifs in transmembrane domains of the human nicotinic acetylcholine receptor. *Sci. Rep.* 1, 69.
- (24) Fantini, J., and Barrantes, F. J. (2009) Sphingolipid/cholesterol regulation of neurotransmitter receptor conformation and function. *Biochim. Biophys. Acta* 1788, 2345–2361.
- (25) Fantini, J., and Yahi, N. (2011) Molecular basis for the glycosphingolipid-binding specificity of  $\alpha$ -synuclein: Key role of tyrosine 39 in membrane insertion. *J. Mol. Biol.* 408, 654–669.
- (26) Mahfoud, R., Garmy, N., Maresca, M., Yahi, N., Puigserver, A., and Fantini, J. (2002) Identification of a common sphingolipid-binding domain in Alzheimer, prion, and HIV-1 proteins. *J. Biol. Chem.* 277, 11292–11296.
- (27) Mason, R. P., Estermyer, J. D., Kelly, J. F., and Mason, P. E. (1996) Alzheimer's disease amyloid beta peptide 25–35 is localized in the membrane hydrocarbon core: X-ray diffraction analysis. *Biochem. Biophys. Res. Commun.* 222, 78–82.
- (28) D'Erico, G., Vitiello, G., Ortona, O., Tedeschi, A., Ramunno, A., and D'Ursi, A. M. (2008) Interaction between Alzheimer's A $\beta$ (25–35) peptide and phospholipid bilayers: the role of cholesterol. *Biochim. Biophys. Acta* 1778, 2710–2716.
- (29) Strandberg, E., and Killian, J. A. (2003) Snorkeling of lysine side chains in transmembrane helices: How easy can it get? *FEBS Lett.* 544, 69–73.
- (30) Zhou, X., and Xu, J. (2012) Free cholesterol induces higher  $\beta$ -sheet content in A $\beta$  peptide oligomers by aromatic interaction with Phe19. *PLoS One* 7, No. e46245.
- (31) Nelson, T. J., and Alkon, D. L. (2007) Protection against  $\beta$ -amyloid-induced apoptosis by peptides interacting with  $\beta$ -amyloid. *J. Biol. Chem.* 282, 31238–31249.
- (32) Kallberg, Y., Gustafsson, M., Persson, B., Thyberg, J., and Johansson, J. (2001) Prediction of amyloid fibril-forming proteins. *J. Biol. Chem.* 276, 12945–12950.
- (33) Fantini, J. (2003) How sphingolipids bind and shape proteins: Molecular basis of lipid-protein interactions in lipid shells, rafts and related biomembrane domains. *Cell. Life Sci.* 60, 1027–1032.
- (34) Ji, S. R., Wu, Y., and Sui, S. F. (2002) Cholesterol is an important factor affecting the membrane insertion of beta-amyloid peptide (A $\beta$  1–40), which may potentially inhibit the fibril formation. *J. Biol. Chem.* 277, 6273–6279.
- (35) Micelli, S., Meleleo, D., Picciarelli, V., and Gallucci, E. (2004) Effect of sterols on beta-amyloid peptide (A $\beta$ 1–40) channel formation and their properties in planar lipid membranes. *Biophys. J.* 86, 2231–2237.
- (36) Yu, X., and Zheng, J. (2012) Cholesterol promotes the interaction of Alzheimer  $\beta$ -amyloid monomer with lipid bilayer. *J. Mol. Biol.* 421, 561–571.
- (37) Harris, J. R., and Milton, N. G. (2010) Cholesterol in Alzheimer's disease and other amyloidogenic disorders. *Subcell. Biochem.* 51, 47–75.
- (38) Kang, J., Lemaire, H. G., Unterbeck, A., Salbaum, J. M., Masters, C. L., Grzeschik, K. H., Multhaup, G., Beyreuther, K., and Müller-Hill, B. (1987) The precursor of Alzheimer's disease amyloid A4 protein resembles a cell-surface receptor. *Nature* 325, 733–736.
- (39) Singh, R. P., Brooks, B. R., and Klauda, J. B. (2009) Binding and release of cholesterol in the Osh4 protein of yeast. *Proteins* 75, 468–477.



(40) Thomsen, R., and Christensen, M. H. (2006) MolDock: A new technique for high-accuracy molecular docking. *J. Med. Chem.* 49, 3315–3321.